TSG-6 Produced by hMSCs Delays the Onset of Autoimmune Diabetes by Suppressing Th1 Development and Enhancing Tolerogenicity

Daniel J. Kota, Lindsey L. Wiggins, Nara Yoon, and Ryang Hwa Lee

Genetic and immunological screening for type 1 diabetes has led to the possibility of preventing disease in susceptible individuals. Here, we show that human mesenchymal stem/stromal cells (hMSCs) and tumor necrosis factor-α–stimulated gene 6 (TSG-6), a protein produced by hMSCs in response to signals from injured tissues, delayed the onset of spontaneous autoimmune diabetes in NOD mice by inhibiting insulitis and augmenting regulatory T cells (Tregs) within the pancreas. Importantly, hMSCs with a knockdown of *tsg-6* were ineffective at delaying insulitis and the onset of diabetes in mice. TSG-6 inhibited the activation of both T cells and antigen-presenting cells (APCs) in a CD44-dependent manner. Moreover, multiple treatments of TSG-6 rendered APCs more tolerogenic, capable of enhancing Treg generation and delaying diabetes in an adoptive transfer model. Therefore, these results could provide the basis for a novel therapy for the prevention of type 1 diabetes. ***Diabetes*** **62:2048–2058, 2013**

Recent advances in the use of genetic and immunological screening for identification of prediabetic patients (1–3) have opened up the opportunity to prevent, delay, or halt disease progression before the diagnosis of diabetes. Based on the success in animal models (4–6), clinical trials of oral or nasal insulin (7,8) and nicotinamide (9,10) have been conducted in humans to prevent type 1 diabetes. However, despite all efforts, these clinical trials have failed to show any improvement in the prevention of type 1 diabetes.

Recently, we found that intravenously administered human mesenchymal stem/stromal cells (hMSCs) were activated to express the anti-inflammatory protein tumor necrosis factor (TNF)-α–stimulated gene 6 (TSG-6), which reduced excessive inflammatory response in the myocardial-infarcted heart in mice (11), chemically and mechanically injured cornea in rodent models (12,13), and zymosan-induced peritonitis in mice (14). Specifically, our recent observation revealed that TSG-6 attenuated zymosan-induced mouse peritonitis by decreasing TLR2-mediated NF-κB signaling in resident macrophages (14). This suppressive effect of TSG-6 on NF-κB signaling could provide the rationale for TSG-6 as a potential therapy for the prevention of type 1 diabetes, since several studies have already shown that inflammation and the innate immune system contribute to induction, amplification, and maintenance of the immune cell infiltrate as well as β-cell destruction during this preclinical period (15–17). Particularly, antigen-presenting cells (APCs) from NOD mice, mainly dendritic cells (DCs) and macrophages, have been shown to secrete substantially elevated levels of interleukin-12 (IL-12) and TNF-α (18,19) due to NF-κB hyperactivity (18,20), which leads to T-helper 1 (Th1) development and overt diabetes (21).

Here, we tested whether a new treatment for the prevention of type 1 diabetes could be developed using TSG-6, which hMSCs produce in response to signals from injured tissues. Our data showed that systemic administration of hMSCs to prediabetic mice delayed the onset of type 1 diabetes in NOD mice in part by secreting TSG-6.

RESEARCH DESIGN AND METHODS

Animals. Female NOD/LtJ (stock 001976), NOD/*scid* (stock 001303), C57BL/6J WT (stock 000664), and CD44 KO mice (stock 005085: B6.Cg-Cd44tm1Hbg/J) from Jackson Laboratory (Bar Harbor, ME) were cared for at Scott & White Department of Comparative Medicine under a protocol approved by the Institutional Animal Care and Use Committee.

hMSC culture. hMSCs were prepared as previously described (11).

Transfections with TSG-6 small interfering RNA. Viable passage 1 hMSCs were used for small interfering RNA (siRNA) transfections. hMSCs were transfected with 20 nmol/L siRNA for *tsg-6* (sc-39819; Santa Cruz Biotechnology, Santa Cruz, CA) or RNAi negative control (Stealth RNAi Negative Control; Life Technologies, Grand Island, NY) according to the manufacturer's protocol using Lipofectamine RNAiMAX (Life Technologies). Six hours later, the medium was replaced with CCM (α-MEM [Life Technologies] containing 17% FBS [lot selected for rapid growth of MSCs; Atlanta Biologicals, Inc., Norcross, GA] and 2 mmol/L L-glutamine [Life Technologies]) lacking antibiotics and hMSCs were incubated for 16–20 h. hMSCs were harvested for RNA isolation according to the manufacturer's instructions (RNeasy Mini Kit; Qiagen, Valencia, CA), and the efficacy of the siRNA on the expression of *tsg-6* was assayed using real-time RT-PCR.

Diabetes incidence study. Blood glucose levels were assessed by tail bleeding according to National Institutes of Health guidelines, and mice were regarded as diabetic if they displayed ≥150 mg/dL fasting or ≥250 mg/dL nonfasting blood glucose for two consecutive readings.

Islet histology. Pancreatic sections (5 μm) were hematoxylin-eosin (H-E) stained (Shandon Rapid Chrome frozen section-staining kit; Thermo Fisher Scientific, Waltham, MA), and islet numbers were quantified relative to pancreatic sections or areas. Insulitis scoring was performed on H-E–stained pancreatic sections. Insulitis scores were graded as follows: grade 0, normal islets; grade 1, mild mononuclear infiltration (<25%) at the periphery; grade 2, 25–50% of the islets infiltrated; grade 3, >50% of the islets infiltrated; grade 4, islets completely infiltrated with no residual parenchyma remaining. At least 20 islets per mouse were analyzed and pooled from sections obtained from different mice. For immunofluorescence, the sections were incubated for 18 h at 4°C with antibodies against mouse insulin (1:800, C27C9; Cell Signaling, Danvers, MA), mouse CD4 (1:100, clone YTS191.1; AbD Serotec, Kidlington, U.K.), and mouse Foxp3 (1:100, clone FJK-16s; eBioscience, San Diego, CA).

Real-time PCR assays. About 200 ng of total RNA from the cell cultures was used to synthesize double-stranded cDNA by reverse transcription (SuperScript III; Life Technologies). cDNA was analyzed by real-time PCR (ABI 7900 Sequence Detector; Applied Biosystems, Carlsbad, CA). The mouse primers and probes (Applied Biosystems; Life Technologies) for assay of mouse-specific transcripts were IL-1β (Mm99999061_mH), IFN-γ (Mm00801778_m1), IL-2

From the Texas A&M Health Science Center, College of Medicine, Institute for Regenerative Medicine at Scott & White, Temple, Texas.
Corresponding author: Ryang Hwa Lee, rlee@medicine.tamhsc.edu.
Received 12 July 2012 and accepted 7 January 2013.
DOI: 10.2337/db12-0931
This article contains Supplementary Data online at http://diabetes.diabetesjournals.org/lookup/suppl/doi:10.2337/db12-0931/-/DC1.

(Mm00434256_m1), IL-12a (Mm00434165_m1), IL-12b (Mm01288992_m1), TNF-α (Mm00443258_m1), TGF-β (Mm00441729_g1), Foxp3 (Mm00475162_m1), and IL-10 (Mm99999062_m1) using Taqman Fast Universal PCR Master Mix (Applied Biosystems; Life Technologies). For relative quantitation of gene expression, mouse-specific GAPDH primers and probe (Mm99999915_g1) were used.

Isolation and activation of splenocytes and T cells. Splenocytes and T cells were cultured in 96-well plates precoated with anti-CD3 Ab (BD Biosciences, Franklin Lakes, NJ) plus anti-CD28 Ab (T-cell cultures only, 2 μg/mL; BD Biosciences) or CD3/CD28 beads (Life Technologies), and splenocytes were also cultured with lipopolysaccharide (LPS, 50–100 ng/mL; Sigma-Aldrich, St. Louis, MO) in 5% heat-inactivated FBS (hFBS; Atlanta Biologicals) plus 100 units/mL penicillin and 100 μg/mL streptomycin (pen/strep; both from Life Technologies) in RPMI (ATCC, Manassas, VA), all with different recombinant human (rh) TSG-6 concentrations or cocultured with mitomycin-treated (2.5 μg/mL for 2 h at 37°C; Roche, Mannheim, Germany) scrambled (Scr) siRNA– or TSG-6 siRNA–transfected hMSCs. MTT assay (Promega, Madison, WI) was performed according to the manufacturer's protocol, and Th1 cytokine expression was detected by real-time PCR or ELISA (R&D Systems) according to the manufacturer's protocol. Apoptotic splenocytes were quantified by fluorescence-activated cell sorter analysis using the Annexin V-FITC Apoptosis Detection Kit plus 7-aminoactinomycin D (7-AAD), both from Sigma-Aldrich.

Western blot and immunoprecipitation. For immunoprecipitation, the pellet was resuspended in 6×10^6 cells/400 μL cell lysis buffer (Cell Signaling, Danvers, MA; Complete Protease Inhibitor Cocktail Tablets; Roche) for 30 min on ice, vortexing every 5 min. Cell lysate was microcentrifuged for 10 min at 14,000*g*, 4°C, and the primary antibody (either anti-mouse CD3ε or anti-mouse Zap-70; Cell Signaling) was added to the supernatant for an overnight 4°C incubation. Next, protein A agarose beads (Cell Signaling) were added and incubated for 3 h at 4°C. The sample was centrifuged for 30 s at 4°C, and the pellet was washed three times with cell lysis buffer, followed by resuspension of the pellet with 3× SDS buffer (Blue Loading Buffer plus Reducing Agent [DTT]; Cell Signaling). For Western blot analysis, whole-cell lysate cell pellets (2×10^6 cells) were resuspended with 50 μL 1× SDS buffer (Cell Signaling), and the sample was sonicated for 10–15 s on ice. Samples (40 μL) from both immunoprecipitated and whole-cell lysate samples were heated to 95–100°C for 5 min and briefly centrifuged. Proteins were electrophoresed on Nu-PAGE SDS-polyacrylamide gels (Life Technologies) and transferred to polyvinylidene difluoride membranes (Life Technologies). The membranes were blocked in 5% nonfat dry milk (Cell Signaling) in TBS buffer (Life Technologies) with 0.1% Tween (Thermo Fisher Scientific) (TBST) and incubated overnight in 5% BSA (Thermo Fisher Scientific) in TBST at 4°C with one of the following primary antibodies: p44/42 MAPK, phospho-p44/42 MAPK, Zap-70, phospho-Zap-70 (Cell Signaling), CD44 (Santa Cruz Biotechnology, Santa Cruz, CA), Lck, LAT, and phospho-LAT (Abcam). Membranes were then washed and incubated with the appropriate horseradish peroxidase–conjugated secondary antibody (Cell Signaling) in 5% nonfat dry milk (Cell Signaling) in TBST for 1 h and washed, and protein signals were detected using an enhanced chemiluminescence system (Versadoc Imaging 4000 MP; Bio-Rad, Hercules, CA).

Generation and activation of bone marrow APCs and TSG-6 bone marrow APCs. Mononuclear cells aseptically flushed from the femurs and tibiae of mice were seeded at 10^6 cells/mL in RPMI containing 10% hFBS plus pen/strep, GM-CSF (20 ng/mL), and IL-4 (10 ng/mL) (both from R&D Systems, Minneapolis, MN). On day 3, additional media was added to the plate. On days 5, 7, and 9, media including floating cells was collected and centrifuged, and cells were resuspended in fresh medium and added back. For TSG-6 bone marrow (BM) APC generation, rh TSG-6 was added at days 0, 3, 5, 7, and 9. Cells were harvested at different time points. Cells were harvested at 8–12 days for CD11c (HL3), CD11b (M1/70), and B220 (RA2-6BR) staining (all from BD Pharmingen, San Jose, CA) or activated with LPS (50 ng/mL; Sigma-Aldrich) for 18 h and stained for CD11c (HL3), CD80 (16-10A1), CD86 (GL1), and CD40 (3/23) expression; Th1 and Th3 cytokines were measured by ELISA (R&D Systems).

NF-κB translocation assay. Control-BM APCs were plated at 10^4 cells/mL in four-well chamber slides (Laboratory-Tek II Chamber Slide; Nalge Nunc; Thermo Fisher Scientific, Waltham, MA) and activated with LPS (50 ng/mL) for 15 min in RPMI with 2% hFBS and stained as previously described (15).

In vivo LPS stimulation. Female NOD, C57BL/6J, and CD44 KO mice were intravenously infused with PBS or LPS (30 μg/mouse), followed by intravenous rh TSG-6 infusion (50 μg/mouse). At 6 h postinjection, RNA was isolated from splenocytes for the detection of Th1 expression. $CD11c^+$ and $CD11b^+$ cells were further magnetically isolated (Miltenyi Biotec, Auburn, CA).

BM APC T-cell cocultures. Control-BM APCs or TSG-6-BM APCs were cocultured in 96-well plates with isolated $CD4^+$ T cells in RPMI with 10% hFBS. On day 4 or 5, Th3 levels on culture supernatants were measured by ELISA (R&D Systems) and the $CD4^+CD25^+Foxp3^+$ regulatory T cell (Treg) population identified by flow cytometry analysis using CD4 (GK1.5), CD25 (7D4), and Foxp3 (3G3) antibodies, all from Miltenyi Biotec.

Generation of Tregs in vivo. TSG-6-BM APCs, control-BM APCs, or vehicle control (Hanks' balanced salt solution [HBSS]) were intravenously infused into female NOD mice. Five days later, splenocytes were isolated and analyzed by flow cytometry.

Diabetes adoptive transfer model. TSG-6-BM APCs, control-BM APCs, rh TSG-6, or vehicle control (200 μL) were intravenously infused immediately after infusion of 10^7 diabetic splenocytes from diabetic female NOD mice into NOD/*scid* mice. Rh TSG-6 was additionally infused 1 week after. Glucose measurements and diabetes incidence were performed as described above.

RESULTS

Intravenously administered hMSCs and TSG-6 delayed onset of autoimmune diabetes in NOD mice. To test whether the administration of hMSCs could delay the onset of type 1 diabetes in a preclinical period, we infused hMSCs to prediabetic female NOD mice. Systemic administration of hMSCs delayed the onset of type 1 diabetes in NOD mice (Fig. 1*A*). To examine hMSC engraftment after intravenous infusion, we screened human cells (11) in pancreas, pancreatic lymph nodes (PLNs), spleen, and lung at 1, 2, 3, and 7 days after intravenous infusion using real-time RT-PCR for human *Gapdh* (Supplementary Table 1). Most of the infused cells were trapped in the lung as shown previously (11). A small number of human cells were found in the spleen at 1 day after intravenous infusion; however, these cells disappeared after 2 days as previously shown (11). To test whether the beneficial effects of hMSCs in the model could be duplicated by the administration of TSG-6, we infused TSG-6 into female NOD mice. Multiple infusions of TSG-6 delayed the onset of diabetes, but two infusions of TSG-6 at ages 10 and 11 weeks had no significant effects (Fig. 1*B*). Islets from untreated mice were extensively infiltrated by lymphoid cells, displayed disrupted structure, and had a reduction of insulin expression (Fig. 1*C*). In contrast, islets from hMSC- and TSG-6–treated mice were free of or displayed moderate insulitis and contained more insulin-positive cells (Fig. 1*C*). In addition, hMSC- and TSG-6–treated mice had more islets (Fig. 1*D*) and less severe insulitis than untreated mice (Fig. 1*E*). The administration of hMSCs or TSG-6 increased $Foxp3^+$ cells in the islets of treated NOD mice (Fig. 1*F* and *G*). Therefore, these data suggest that the administration of hMSCs and TSG-6 to prediabetic mice delays the onset of type 1 diabetes by reducing insulitis in islets and preserving insulin-positive islets.

Administration of hMSCs reduced insulitis by secreting TSG-6 in NOD mice. To determine the progression of islet mass loss and insulitis in NOD mice and the effect of hMSC administration on such events, we analyzed islet numbers and insulitis in HBSS- and hMSC-treated mice (Fig. 2*A*). The number of islets started to significantly decrease after 12 weeks of age in the HBSS-treated group (Fig. 2*B*). In mice that received two infusions of hMSCs at 10 and 11 weeks of age, however, islet numbers remained significantly higher at 12 weeks when compared with age-matched HBSS control (Fig. 2*B*). There was no significant difference in islet numbers between the hMSC- and HBSS-treated groups of 14-week-old mice (Fig. 2*B*). However, the hMSC-treated group showed significant differences in insulitis at all ages tested, and earlier infusions of hMSCs, before insulitis was well established, more effectively delayed insulitis in NOD mice (Fig. 2*C*). To determine whether the administration of hMSCs to prediabetic mice delays insulitis in NOD mice by secreting TSG-6, we infused TSG-6 siRNA–transfected

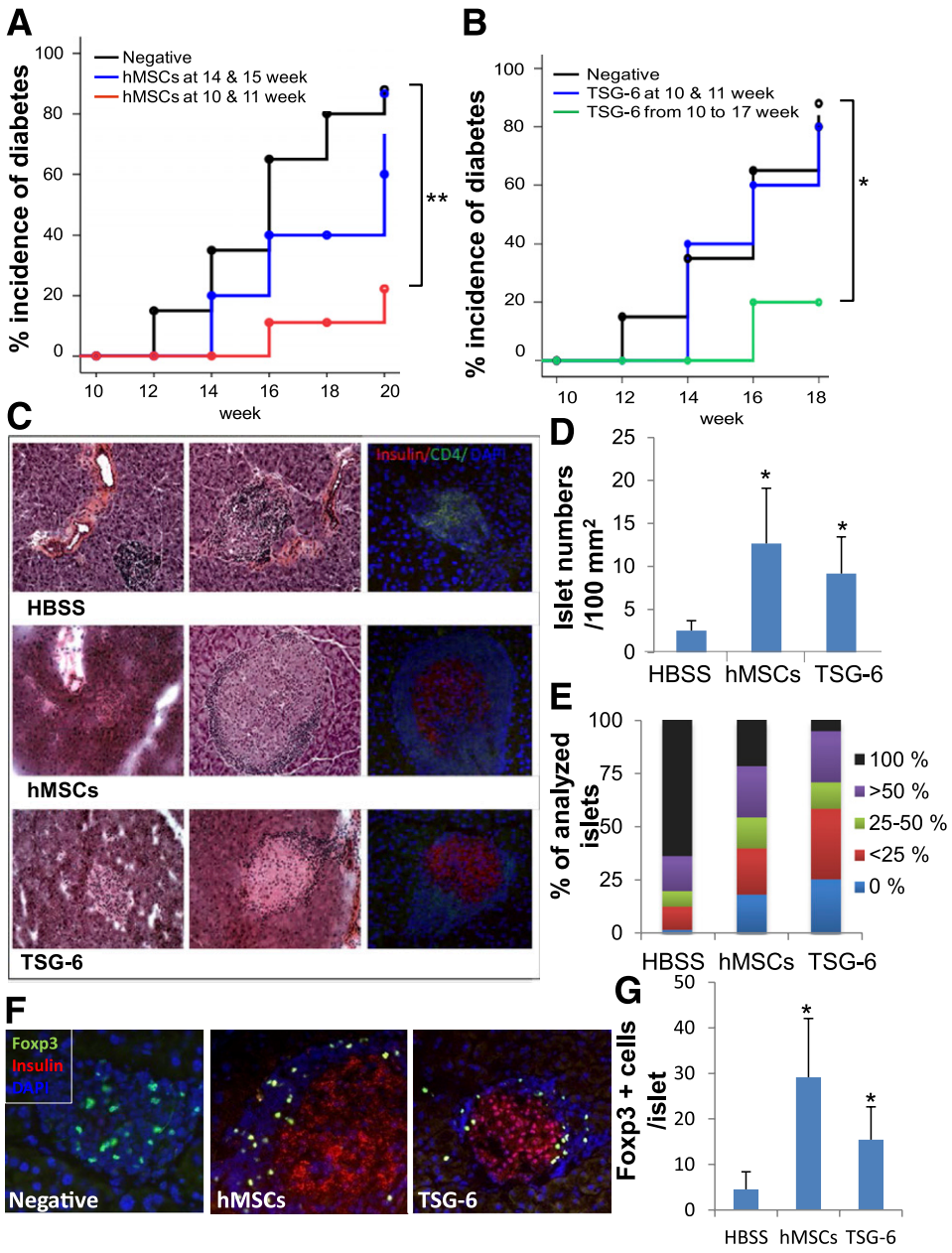

FIG. 1. Systemic administration of hMSCs or TSG-6 delayed the onset of diabetes in NOD mice. *A* and *B*: Diabetes incidence. Negative, HBSS infused (n = 10) at 10 and 11 weeks of age; hMSCs at 14 and 15 weeks, hMSC infused (2×10^6, n = 10) at 14 and 15 weeks of age; hMSCs at 10 and 11 weeks, hMSC infused (2×10^6, n = 10) at 10 and 11 weeks of age; TSG-6 at 10 and 11 weeks, TSG-6 infused (50 μg/mouse, n = 10) at 10 and 11 weeks of age; TSG-6 from 10 to 17 weeks, TSG-6 infused (50 μg/mouse, n = 5) from 10 to 17 weeks of age. *$P < 0.05$, **$P < 0.005$ by Kaplan-Meier estimator. *C–G*: HBSS, HBSS infused (n = 10) at 10 and 11 weeks of age; hMSCs, hMSC infused (2×10^6, n = 10) at 10 and 11 weeks of age; TSG-6, TSG-6 infused (50 μg/mouse, n = 5) from 10 to 17 weeks of age. *C*: End point–representative H-E and immunofluorescence staining for CD4 and insulin. *D* and *E*: Islet number per area and insulitis characterization (n = 3 or 4). *F*: Representative immunofluorescence staining for Foxp3 and insulin. *G*: Foxp3$^+$ quantification per islet (n = 3 or 4). Values for islet numbers and Foxp3 are means ± SD. *$P < 0.05$ by two-tailed Student t test.

hMSCs or TSG-6 at 10 and 11 weeks of age. Transient transfection of hMSCs with TSG-6 siRNA (Supplementary Fig. 1*A*) abrogated the effects (Fig. 2*D* and *E*) and TSG-6 duplicated the effects of hMSC (Fig. 2*F* and *G*). Most importantly, TSG-6 siRNA–transfected hMSCs (Supplementary Table 1 and Supplementary Fig. 1*B*) have no statistically significant effect in delaying diabetes in an adoptive transfer model (Fig. 2*H*). Therefore, these data strongly suggested that infusion of hMSCs delays the onset of type 1 diabetes in NOD mice in part by secreting TSG-6.

TSG-6 suppressed expression of Th1 cytokines in NOD mice. To test whether hMSCs delayed insulitis by inhibiting the development of Th1 cells, which are implicated in the destruction of insulin-producing β-cells (22), we infused hMSCs to prediabetic NOD mice at 10 and 11 weeks of age and analyzed Th1 cytokine expression in the spleen of these animals at 12 weeks of age. As shown in Fig. 3*A*, the administration of hMSCs significantly decreased gene expression of *il-12*, *ifn-γ*, *il-2*, and *il-1β* in hMSC-treated mice compared with age-matched HBSS-treated NOD mice. The administration of hMSCs and TSG-6

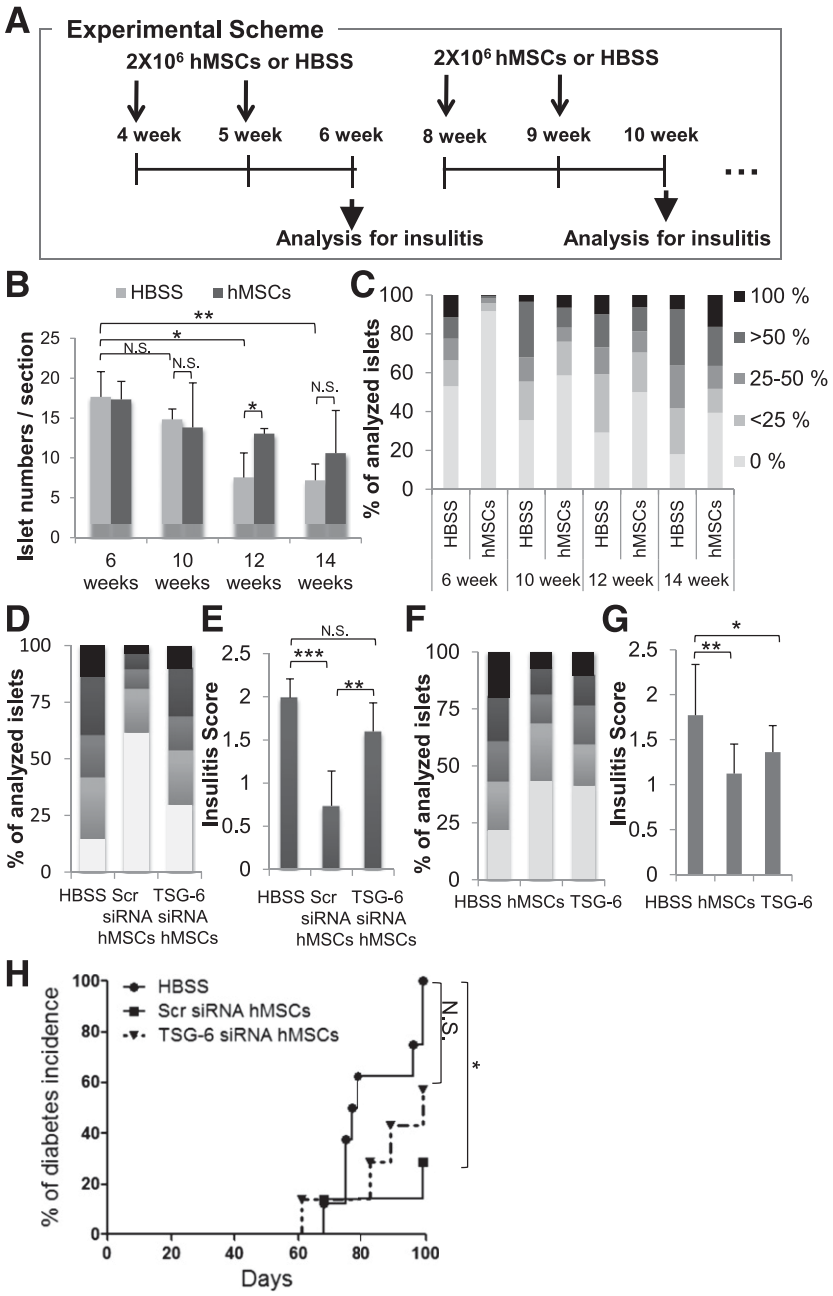

FIG. 2. Administered hMSCs reduced insulitis by secreting TSG-6 in NOD mice. *A*: Experimental scheme. Insulitis was analyzed in the pancreas after weekly two-time infusions of HBSS or hMSCs at various ages. Islet number per pancreatic section (*B*) and insulitis characterization (*C*) from HBSS- ($n = 3$) or hMSC-infused mice (2×10^6, $n = 3$) at various ages. Values are means ± SD. *$P < 0.05$; **$P < 0.005$. NS, not significant by two-tailed Student *t* test. Insulitis characterization (*D*) and insulitis score (*E*) from 12-week-old mice HBSS ($n = 8$), Scr siRNA hMSC (2×10^6, $n = 6$), or TSG-6 siRNA hMSC infused (2×10^6, $n = 6$) at 10 and 11 weeks of age. Insulitis characterization (*F*) and insulitis score (*G*) from 12-week-old mice HBSS ($n = 8$), hMSC (2×10^6, $n = 6$), or TSG-6 infused (50 μg, $n = 6$) at 10 and 11 weeks of age. At least 20 individual islets per mouse were examined for insulitis characterization and score. Insulitis score values are means ± SD. *$P < 0.05$, **$P < 0.005$, ***$P < 0.0005$ by one-way ANOVA. *H*: Diabetes incidence after diabetogenic splenocytes (10^7 cells/mouse) pooled from 11-week-old female NOD mice that were intravenously cotransferred with HBSS ($n = 8$), Scr siRNA–transfected hMSCs (1×10^6, $n = 7$), or TSG siRNA–transfected hMSCs (1×10^6, $n = 7$). *$P < 0.05$ by Kaplan-Meier estimator.

weekly at 4 and 5 weeks of age, before insulitis was well established, also reduced the expression of Th1 cytokines in the PLNs of NOD mice (Fig. 3*B*). Most importantly, the gene expression of *il-12*, released from APCs, which are mainly macrophages and DCs and are critically involved in the development of Th1 cells (23,24), was significantly decreased in hMSC- and TSG-6–treated mice. These data suggested that TSG-6 either directly suppresses Th1 polarization or indirectly decreases *il-12* expression levels in APCs, therefore inhibiting the expression of Th1 cytokines.

TSG-6 directly suppressed Th1 polarization. To determine the extent to which TSG-6 directly suppressed Th1 polarization, splenocytes from NOD mice were activated in vitro in the presence of TSG-6 or hMSCs transfected with siRNA against *tsg-6*. TSG-6 suppressed proliferation of

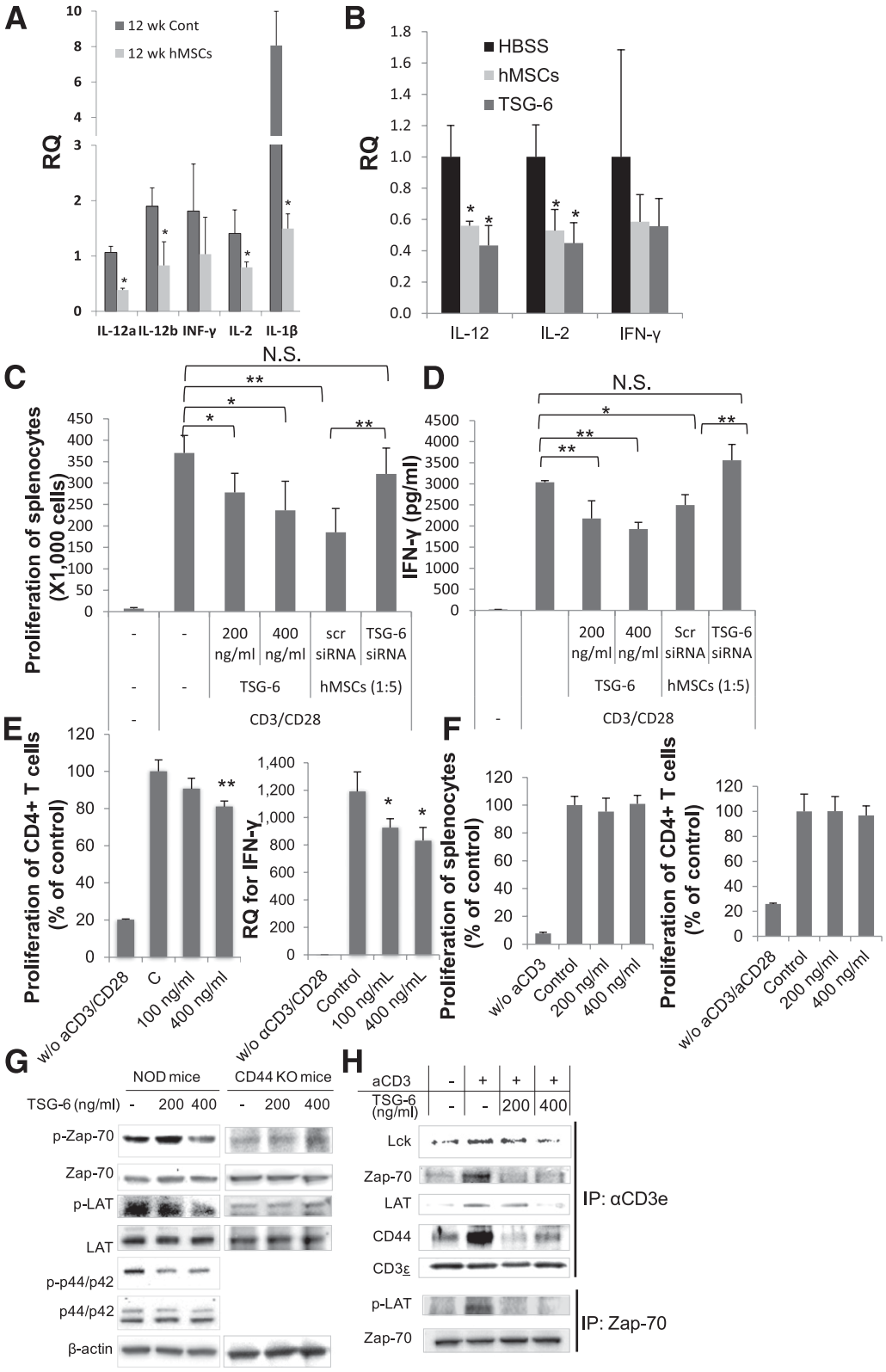

FIG. 3. hMSCs or TSG-6–suppressed Th1 cytokine expression in vivo and in vitro. *A*: Splenic Th1 expression from 12-week-old mice HBSS ($n = 3$) or hMSC infused (2×10^6, $n = 3$) at 10 and 11 weeks of age. Values are means ± SD. *$P < 0.05$ by two-tailed Student t test. *B*: Th1 expression in PLNs from 6-week-old mice HBSS ($n = 3$) or hMSC infused (2×10^6, $n = 3$) at 4 and 5 weeks of age. RQ, relative quantification. MTT assay (*C*) and Th1 expression (*D*) after 72 h of splenocyte cultures (1×10^6/mL) in the presence of TSG-6 or hMSCs transfected with Scr or TSG-6 siRNA (hMSCs, splenocytes = 1:5). *E*: MTT assay after 72 h and Th1 expression after 24 h from CD4$^+$ T cells (5×10^5/mL) in the presence of TSG-6. *F*: MTT assay after 72 h from CD44 KO splenocytes (2.5×10^6/mL) or CD44 KO CD4$^+$ T cells (1×10^6 cells/mL) in the presence of TSG-6. Values are means ± SD. *$P < 0.05$, **$P < 0.005$ by one-way ANOVA. *G*: Western blot of cell lysate 15 min after CD4$^+$ T cell (1×10^6/mL) activation in 24-well plates precoated with anti-CD3 (2 μg/mL) in the presence of TSG-6. *H*: Immunoprecipitation with TCR (CD3ε) or Zap-70 from cell lysate.

splenocytes (Fig. 3*C*), accompanied by suppression of Th1-related cytokines (Fig. 3*D* and Supplementary Fig. 2). This effect was not due to cell death (Supplementary Fig. 3). Importantly, suppression of Th1 development was ineffective when splenocytes were cocultured with TSG-6 siRNA–transfected hMSCs (Fig. 3*C* and *D* and Supplementary Fig. 2). Previously, TSG-6 was shown to modulate the interaction of hyaluronic acid (HA) with the cell surface receptor CD44 (25), and we also showed that the inhibitory effects of TSG-6 on NF-κB signaling were dependent on CD44 expression (14). Therefore, we tested the hypothesis that the inhibitory effects of TSG-6 were dependent on the expression of CD44 on T cells. TSG-6 had no effect on the proliferation of splenocytes or $CD4^+$ cells isolated from transgenic mice with inactivated alleles for CD44 (Fig. 3*F*), whereas TSG-6 suppressed activation of $CD4^+$ cells isolated from NOD mice (Fig. 3*E*). Western blots revealed that TSG-6 suppressed phosphorylation of Zap-70, LAT, and p42MAPK, key molecules downstream on the CD3 activation signaling cascade in $CD4^+$ T cells from NOD mice (26) (Fig. 3*G*), but not CD44 knockout mice (Fig. 3*G*). Furthermore, when Triton X-100 lysates of $CD4^+$ T cells were immunoprecipitated with anti-TCR (CD3ε) or Zap-70 after CD3 stimulation with or without TSG-6, only a small amount of coprecipitated Lck, CD44, Zap-70, and LAT was detected in TSG-6–treated T cells compared with control (Fig. 3*H*). These data suggest that TSG-6 directly suppressed TCR signaling by inhibiting coalescence of the TCR microdomains, and this inhibitory effect of TSG-6 was dependent on CD44.

TSG-6 suppressed APC activation. To determine the extent to which TSG-6 suppressed APC activation, we tested the effect of TSG-6 on the activation of APCs both in vitro and in vivo. We first assessed *il-12b* and *tnf-α* expression in splenocytes after intravenous LPS exposure in vitro. Splenocytes were treated with LPS with or without TSG-6, and proliferation and cytokine profile were assessed. TSG-6 suppressed *il-12b* gene expression at 4 and 6 h (Fig. 4*A*), inhibited NF-κB translocation (Supplementary Fig. 4), splenocyte proliferation, and secretion of IFN-γ after 3 days (Supplementary Fig. 5), and inhibited expression of CD40 (Fig. 4*B*), CD80, and CD86 (Supplementary Table 2*A*) at 20 h. Next, coadministration of TSG-6 was able to suppress the expression of *il-12b*, *tnf-α*, and *ifn-γ* in the spleen of LPS-treated animals (Fig. 4*C*). Further magnetic sorting of TSG-6–treated mouse splenocytes revealed the capacity of TSG-6 to substantially suppress *il-12b* and *tnf-α* expression from the $CD11c^+$ and $CD11b^+$ populations, respectively (Fig. 4*D*). Importantly, infusion of TSG-6 was ineffective in *cd44* knockout mice after intravenous LPS stimulation (Fig. 4*E*), consistent with our previous observations that the interaction of TSG-6 with CD44 decreases the translocation of NF-κB in macrophages after zymosan stimulation (14). Since the effects of TSG-6 are dependent on the interactions between CD44 and HA, it is possible that an increased availability of HA in vivo enhances TSG-6 therapeutic effects. This suppressive effect of TSG-6 on NF-κB signaling, along with the reduced levels of the costimulatory molecule CD40 and the cytokines IL-12 and TNF-α, provided more supporting evidence that TSG-6 affects the APC phenotype and thereby suppresses Th1 development.

TSG-6 promoted tolerance in APCs and thereby induced Treg cells. To determine the extent to which TSG-6 promotes APC-mediated tolerance, APCs were generated from BM-derived precursors differentiated in the presence of recombinant murine GM-CSF and IL-4 with TSG-6 (TSG-6-BM APCs) or without TSG-6 (control-BM APCs). TSG-6-BM APCs showed lower expression levels of costimulatory molecules CD40 (Fig. 5*A*), CD80, and CD86 (Supplementary Table 2*B*) compared with control-BM APCs after LPS stimulation. In addition, TSG-6-BM APCs secreted lower levels of activating IL-12 cytokine and higher levels of Th1 inhibitory cytokines IL-10 and TGF-β compared with control-BM APCs after LPS stimulation (Fig. 5*B*). These results led us to further investigate the immunoregulatory properties of the TSG-6-BM APC. The number of the mouse $CD11c^+B220^+CD8\alpha^+$ plasmacytoid dendritic subtype (27) was increased in TSG-6-BM APCs (Fig. 5*C*). To evaluate the effect of TSG-6-BM APCs on the T-lymphocyte phenotype, 4-day cocultures of TSG-6-BM APCs with $CD4^+$ naïve T lymphocytes were performed. As expected, TSG-6-BM APCs were able to generate significantly higher numbers of $CD4^+CD25^+Foxp3^+$ Tregs in vitro (Fig. 6*A*), and levels of the anti-inflammatory cytokine TGF-β were increased in the cocultures with TSG-6-BM APC (Fig. 6*B*). In vivo, TSG-6-BM APCs increased the number of $CD4^+CD25^+Foxp3^+$ Tregs in the spleen of 5-week-old NOD mice 5 days after intravenous infusion (Fig. 6*C* and *D*). Therefore, our results suggest that TSG-6 generated immune tolerance through modulation of the APC phenotype. Finally, to further confirm whether the suppressive effects exerted by TSG-6 and TSG-6-BM APCs on Th1 development could be translated into a T-cell transfer model of diabetes, isolated diabetogenic splenocytes from female NOD mice were adoptively cotransferred into female immune-deficient NOD/*scid* in combination with TSG-6 or TSG-6-BM APCs. Both treatments were able to delay diabetes in recipient NOD/*scid* mice (Fig. 6*E*) and increase expressions of *foxp3* and *il-10* in recipient splenocytes (Fig. 6*F* and *G*), providing further supporting evidence for the therapeutic potential of TSG-6.

DISCUSSION

Our data provide several possible mechanisms whereby TSG-6 suppresses T-cell development into a Th1 phenotype (Supplementary Fig. 6). First, TSG-6 may suppress Th1 development either by direct inhibition of T-cell activation or indirectly through suppression of APC activation. In our study, splenocytes and $CD4^+$ T cells isolated from NOD mice subsequently activated in vitro in the presence of TSG-6 displayed suppressed proliferation capacity, along with significant inhibition of the CD3 and CD28 activation signaling cascade and IFN-γ secretion. In addition, TSG-6 was able to suppress IL-12 and TNF-α levels in APCs after LPS activation through inhibition of NF-κB translocation to the nuclei. Interestingly, CD40 expression, a critical step in the final maturation of DCs into a fully competent APC (28) and essential for IL-12 production (29), and other costimulatory molecules were downregulated by TSG-6. Our results are in accordance with our previous observations (14) that TSG-6 decreased zymosan/TLR2-mediated nuclear translocation of NF-κB in resident macrophages. The suppressive effects of TSG-6 on NF-κB signaling may explain how TSG-6 suppressed Th1 development, since Th1 polarization and APC activation require the activation of NF-κB signaling (20). NF-κB signaling is an essential component for the T-cell activation mechanism in response to engagement of CD3 and CD28 and subsequently induces proliferation and IL-2 production (30,31). Furthermore, APCs from NOD mice,

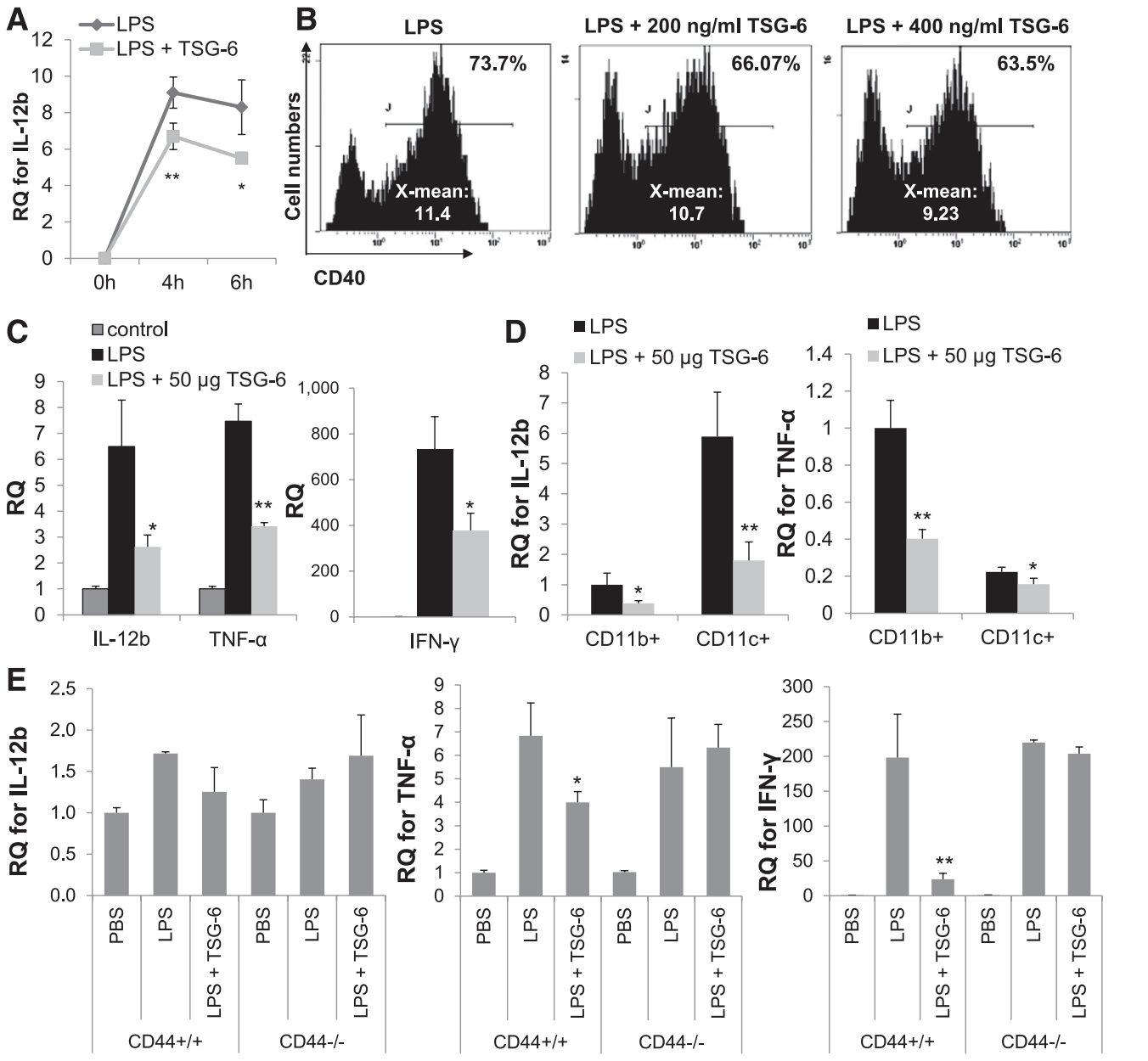

FIG. 4. TSG-6 suppressed APC activation in vitro and in vivo. Splenocytes were activated with LPS (100 ng/mL) in vitro in the presence of TSG-6. *A*: *il-12b* expression 4 and 6 h after activation. Values are means ± SD (n = 3; *P < 0.05, **P < 0.005 by two-tailed Student t test). *B*: CD40 expression 18 h after LPS (100 ng/mL) activation of APC (5×10^5 cells/mL) in the presence of TSG-6. *C*: Splenic *il-12b*, *tnf-α*, and *ifn-γ* expression 6 h in 4-week-old female NOD mice that were intravenously injected with LPS (30 µg/mouse) immediately followed by vehicle control PBS (n = 4) or TSG-6 (50 µg/mouse, n = 3). *D*: *il-12b* and *tnf-α* expression of magnetically sorted $CD11b^+$ and $CD11c^+$ cells from *C*. *E*: Splenic *il-12b*, *tnf-α*, and *ifn-γ* expression 6 h after 8-week-old male WT and CD44 KO mice were intravenously injected with LPS (30 µg/mouse) immediately followed by vehicle control HBSS (n = 4) or TSG-6 (50 µg/mouse, n = 3). Values are means ± SD (*P < 0.05, **P < 0.005 by two-tailed Student t test). RQ, relative quantification.

mainly DCs and macrophages, have also been shown to display NF-κB hyperactivity (18), leading to abnormal levels of IL-12 and TNF-α secretion (18,19). IL-12, in particular, plays a critical role in the development of Th1 cells (23,24), as IL-12 antagonists (32) and administration of IL-12 (33) have been shown to inhibit and accelerate diabetes in NOD mice, respectively. Notably, macrophage depletion (15) and NF-κB–deficient DCs (34) have been shown to prevent diabetes in NOD mice, reinforcing the importance of these immune cells in the pathogenesis of type 1 diabetes.

Our study also demonstrated that this suppressive effect of TSG-6 on T cells, splenocytes, and APCs was dependent on CD44 expression. These results are consistent with the previous observations that the interaction of TSG-6 with CD44 was essential for decreasing zymosan/TLR2-mediated stimulation of NF-κB signaling (14). In TCR/CD3-mediated T-cell activation, CD44 has been shown to function as a costimulatory molecule, leading to enhanced proliferation and cytokine release (35). Cross-linking CD44 by small HA fragments leads to coalescence of the TCR microdomains, because CD44 selectively associates with active Src family protein tyrosine kinases Lck and Fyn (36), which are recruited to the TCR and then phosphorylate and activate Zap-70 during initial canonical

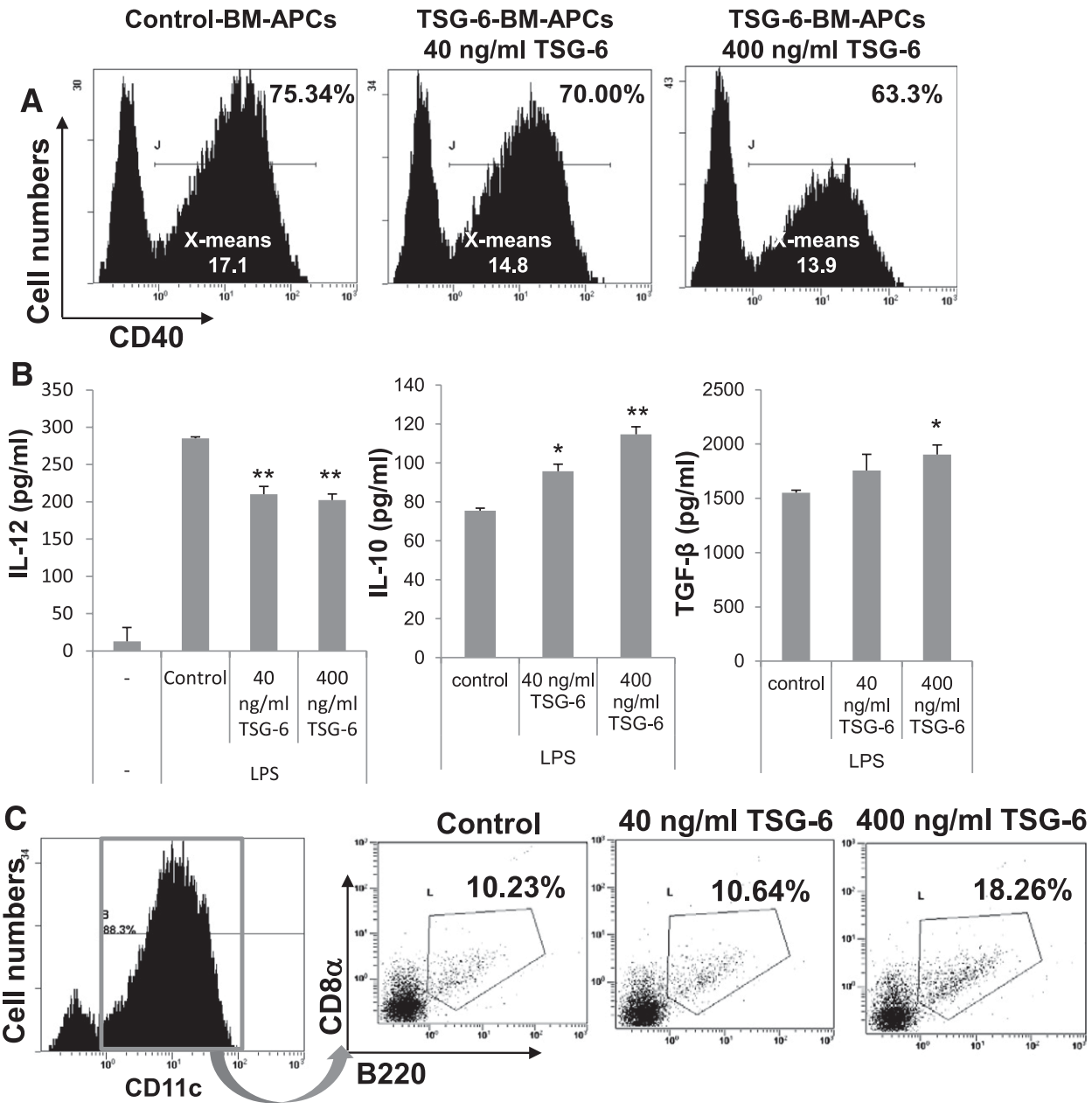

FIG. 5. TSG-6–generated tolerogenic APCs. Expression of CD40 (*A*) and IL-12p70, IL-10, and TGF-β (*B*) of control-BM APCs (5×10^5 cells/mL) and TSG-6-BM APCs (5×10^5 cells/mL) at 18 h after LPS activation (50 ng/mL). Values are means ± SD ($n = 3$; *$P < 0.05$, **$P < 0.005$ by two-tailed Student t test). *C*: $CD11c^+B220^+$ flow cytometry analysis of TSG-6-BM APCs after 9 days.

TCR stimulation (37). Subsequently, Zap-70 phosphorylates T-cell–specific adapters, such as LAT and SLP-76, leading to the recruitment and activation of other kinase families and enzymes, resulting in secondary messenger generation and culminating in T-cell activation (37). However, it has been suggested that polyvalent interaction between polymeric HA and CD44 could possibly prevent coalescence of the TCR microdomains and activation of the associated kinases by inhibiting Lck recruitment to the TCR microdomain (38). Since TSG-6 is implicated in inflammation by stabilizing cellular coats by cross-linking HA chains (39), TSG-6 may keep the polyvalent binding of CD44-HA and thereby inhibit coalescence of the TCR microdomains. Our data also demonstrated that TSG-6 prevents Lck, Zap-70, and LAT from being targeted to the TCR microdomain and thereby abrogated the signaling via TCR.

Second, multiple treatments of TSG-6 may induce regulatory mechanisms, which probably lead to an overall inhibition of the immune system toward a Th1 phenotype by skewing of the immune response toward a Th3, tolerogenic phenotype. Recently, there has been a great interest in regulatory mechanisms for the treatment of type 1 diabetes (40). It has been suggested that the administration of MSCs exerts immune modulation effects in diabetes models associated with an increase in the frequency of $CD4^+CD25^+Foxp3^+$ Tregs (41,42). In our study, we also showed that hMSC- and TSG-6–treated mice maintained Tregs in the islets compared with control mice. Furthermore, we provided supporting evidence that APCs generated in the presence of TSG-6 displayed elevated levels of the Th1 inhibitory cytokines TGF-β and IL-10 and enhanced proportions of the $CD11c^+B220^+$ plasmacytoid

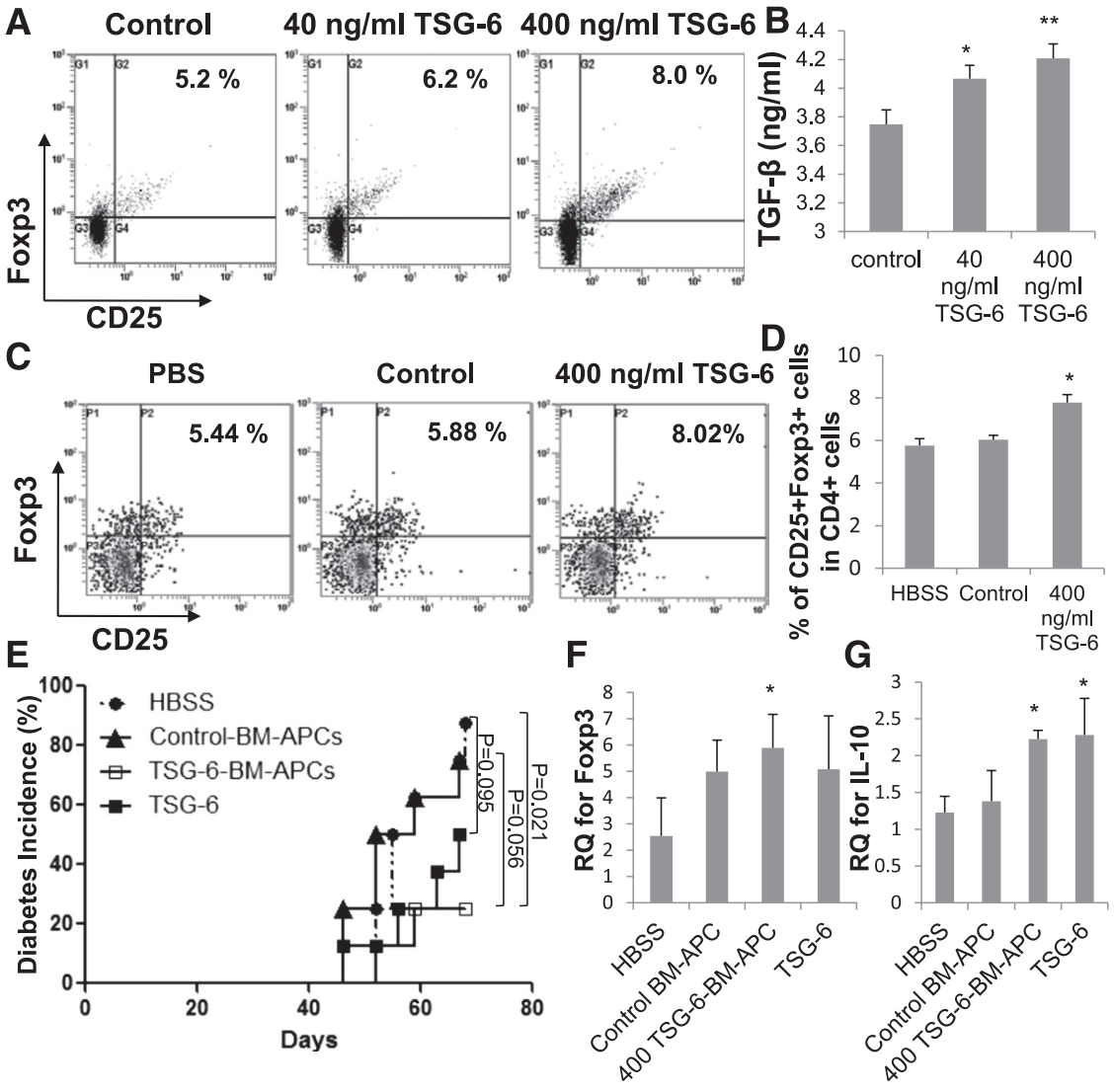

FIG. 6. TSG-6-BM APCs delayed diabetes in an adoptive transfer model. Treg flow analysis (*A*) and TGF-β expression (*B*) 4 days after TSG-6-BM APC (400 ng/mL, 5 × 10^5 cells/mL) and $CD4^+$ T-cell (10^6 cells/mL) cocultures. Splenic Treg representative flow cytometry analysis (*C*) and quantification (*D*) 5 d after vehicle control (PBS, *n* = 4), control-BM APCs (control, 1 × 10^6, *n* = 3), or TSG-6-BM APCs (400 ng/mL, 1 × 10^6, *n* = 3) were intravenously infused in 5-week-old female NOD mice. Values are means ± SD. **P* < 0.05, ***P* < 0.005 by two-tailed Student *t* test. *E*: Diabetes incidence after diabetogenic splenocytes (10^7 cells/mouse) pooled from 11-week-old female NOD mice that were cotransferred with control-BM APCs (10^6 cells/mouse, *n* = 8), TSG-6-BM APCs (10^6 cells/mouse, *n* = 8), TSG-6 (50 μg/mouse, *n* = 8), or vehicle control (HBSS, *n* = 8). TSG-6–treated animals received an additional intravenous infusion of TSG-6 (50 μg/mouse) 1 week posttransfer. HBSS vs. TSG-6-BM APCs, *P* = 0.021; control-BM APCs vs. TSG-6-BM APCs, *P* = 0.056; HBSS vs. TSG-6, *P* = 0.095 by Kaplan-Meier estimator. *foxp3* (*F*) and *il-10* (*G*) expression in splenocytes isolated from mice from *E* (*n* = 3–5) at 70 days. Values are means ± SD. **P* < 0.05 by two-tailed Student *t* test. RQ, relative quantification.

dendritic subtype (27), which have been shown to increase Treg cells and prevent diabetes in animal models (43). In our study, TSG-6-BM APCs were also able to generate significantly higher numbers of $CD4^+CD25^+Foxp3^+$ Tregs both in vitro and in vivo. Finally, TSG-6-BM APCs were able to delay the onset of diabetes when cotransferred with diabetogenic splenocytes in an adoptive diabetic transfer model. TSG-6 also showed the great potential in delaying the onset of diabetes in recipient mice, although the tendency for delay was not statistically significant in the TSG-6 treatment group. The maximal effective dose and injection schedule of TSG-6 need to be optimized in future studies.

A previous study by Fiorina et al. (42) involving the use of MSCs and an experimental model of diabetes showed that mouse MSCs generated tumors after in vivo administration. It is critically important and noteworthy that mouse MSCs significantly differ from other species, in particular humans, in many ways, including heavy hematopoietic contamination in the initial culture, different culture conditions, and, most importantly, genomic instability that allows them to proliferate and become tumorigenic (44). Moreover, Fiorina et al. observed that only mice treated with NOD-derived MSCs, but not BALB/c-derived MSCs, developed neoplasia, which the authors attribute to the fact that inbred mice such as NOD have been shown to carry various genetic abnormalities and are prone to developing lymphoid tumors.

There was a difference in terms of efficacy between MSCs and TSG-6 in delaying the onset of diabetes in NOD mice (Fig. 1*A* and *B*). We speculate that the degree of

biological activity of the commercial TSG-6 differs from the TSG-6 generated in vivo by hMSCs due to potentially different posttranslational modifications. Moreover, other reports suggested that the anti-inflammatory or immunesuppressive activity of MSCs was explained by the cells expressing PGE2 (45), IDO (46), TGF-β1 (47), IL-1 receptor antagonist (48), or the soluble TNF receptor 1 (49). Therefore, it is apparent that MSCs can produce a variety of anti-inflammatory factors in addition to TSG-6. The results presented here do not rule out the effects from additional anti-inflammatory factors produced by hMSCs, but the data from the experiments with TSG-6 siRNA and TSG-6 demonstrate that TSG-6 made a major contribution to the decreased insulitis observed in the pancreas and Th1 development and the delayed the onset of diabetes in NOD mice.

Research in the field of type 1 diabetes within the last 30 years has shifted our understanding of pathogenesis from an acute to a chronic autoimmune disease (3), in which β-cell mass progressively decreases before the development of clinically symptomatic diabetes, a time when >70% of the β-cell mass has already been destroyed (50) and there is insufficient insulin secretion to maintain glucose homeostasis. Therefore, prevention of type 1 diabetes manifestation will have a greater impact than a treatment-focused approach. Our results suggest that TSG-6 could *1*) provide a novel therapy for disease prevention in susceptible individuals at high risk of developing type 1 diabetes, and *2*) replace the current efforts of cell therapies with more practical and less expensive protein therapy for the prevention of type 1 diabetes.

ACKNOWLEDGMENTS

This work was supported by a grant from the Juvenile Diabetes Research Foundation (5-2011-426).

No potential conflicts of interest relevant to this article were reported.

D.J.K. and R.H.L. designed and performed the research, analyzed data, and wrote the paper. L.L.W. and N.Y. performed research. R.H.L. is the guarantor of this work and, as such, had full access to all the data in the study and takes responsibility for the integrity of the data and the accuracy of the data analysis.

REFERENCES

1. Gorus FK, Pipeleers DG; Belgian Diabetes Registry. Prospects for predicting and stopping the development of type 1 of diabetes. Best Pract Res Clin Endocrinol Metab 2001;15:371–389
2. Bingley PJ, Bonifacio E, Gale EA. Can we really predict IDDM? Diabetes 1993;42:213–220
3. Sherr J, Sosenko J, Skyler JS, Herold KC. Prevention of type 1 diabetes: the time has come. Nat Clin Pract Endocrinol Metab 2008;4:334–343
4. Atkinson MA, Maclaren NK, Luchetta R. Insulitis and diabetes in NOD mice reduced by prophylactic insulin therapy. Diabetes 1990;39:933–937
5. Zhang ZJ, Davidson L, Eisenbarth G, Weiner HL. Suppression of diabetes in nonobese diabetic mice by oral administration of porcine insulin. Proc Natl Acad Sci USA 1991;88:10252–10256
6. O'Brien BA, Harmon BV, Cameron DP, Allan DJ. Nicotinamide prevents the development of diabetes in the cyclophosphamide-induced NOD mouse model by reducing beta-cell apoptosis. J Pathol 2000;191:86–92
7. Harrison LC, Honeyman MC, Steele CE, et al. Pancreatic beta-cell function and immune responses to insulin after administration of intranasal insulin to humans at risk for type 1 diabetes. Diabetes Care 2004;27:2348–2355
8. Skyler JS, Krischer JP, Wolfsdorf J, et al. Effects of oral insulin in relatives of patients with type 1 diabetes: The Diabetes Prevention Trial—Type 1. Diabetes Care 2005;28:1068–1076
9. Gale EA, Bingley PJ, Emmett CL, Collier T; European Nicotinamide Diabetes Intervention Trial (ENDIT) Group. European Nicotinamide Diabetes Intervention Trial (ENDIT): a randomised controlled trial of intervention before the onset of type 1 diabetes. Lancet 2004;363:925–931
10. Kolb H, Burkart V. Nicotinamide in type 1 diabetes. Mechanism of action revisited. Diabetes Care 1999;22(Suppl. 2):B16–B20
11. Lee RH, Pulin AA, Seo MJ, et al. Intravenous hMSCs improve myocardial infarction in mice because cells embolized in lung are activated to secrete the anti-inflammatory protein TSG-6. Cell Stem Cell 2009;5:54–63
12. Oh JY, Roddy GW, Choi H, et al. Anti-inflammatory protein TSG-6 reduces inflammatory damage to the cornea following chemical and mechanical injury. Proc Natl Acad Sci USA 2010;107:16875–16880
13. Roddy GW, Oh JY, Lee RH, et al. Action at a distance: systemically administered adult stem/progenitor cells (MSCs) reduce inflammatory damage to the cornea without engraftment and primarily by secretion of TNF-α stimulated gene/protein 6. Stem Cells 2011;29:1572–1579
14. Choi H, Lee RH, Bazhanov N, Oh JY, Prockop DJ. Anti-inflammatory protein TSG-6 secreted by activated MSCs attenuates zymosan-induced mouse peritonitis by decreasing TLR2/NF-{kappa}B signaling in resident macrophages. Blood 2011;118:330–338
15. Jun HS, Yoon CS, Zbytnuik L, van Rooijen N, Yoon JW. The role of macrophages in T cell-mediated autoimmune diabetes in nonobese diabetic mice. J Exp Med 1999;189:347–358
16. Dahlén E, Dawe K, Ohlsson L, Hedlund G. Dendritic cells and macrophages are the first and major producers of TNF-alpha in pancreatic islets in the nonobese diabetic mouse. J Immunol 1998;160:3585–3593
17. Hutchings P, Rosen H, O'Reilly L, Simpson E, Gordon S, Cooke A. Transfer of diabetes in mice prevented by blockade of adhesion-promoting receptor on macrophages. Nature 1990;348:639–642
18. Poligone B, Weaver DJ Jr, Sen P, Baldwin AS Jr, Tisch R. Elevated NF-kappaB activation in nonobese diabetic mouse dendritic cells results in enhanced APC function. J Immunol 2002;168:188–196
19. Alleva DG, Johnson EB, Wilson J, Beller DI, Conlon PJ. SJL and NOD macrophages are uniquely characterized by genetically programmed, elevated expression of the IL-12(p40) gene, suggesting a conserved pathway for the induction of organ-specific autoimmunity. J Leukoc Biol 2001;69:440–448
20. Liu J, Beller D. Aberrant production of IL-12 by macrophages from several autoimmune-prone mouse strains is characterized by intrinsic and unique patterns of NF-kappa B expression and binding to the IL-12 p40 promoter. J Immunol 2002;169:581–586
21. Csorba TR, Lyon AW, Hollenberg MD. Autoimmunity and the pathogenesis of type 1 diabetes. Crit Rev Clin Lab Sci 2010;47:51–71
22. Yoon JW, Jun HS. Autoimmune destruction of pancreatic beta cells. Am J Ther 2005;12:580–591
23. Abbas AK, Murphy KM, Sher A. Functional diversity of helper T lymphocytes. Nature 1996;383:787–793
24. Seder RA, Gazzinelli R, Sher A, Paul WE. Interleukin 12 acts directly on CD4+ T cells to enhance priming for interferon gamma production and diminishes interleukin 4 inhibition of such priming. Proc Natl Acad Sci USA 1993;90:10188–10192
25. Lesley J, Gál I, Mahoney DJ, et al. TSG-6 modulates the interaction between hyaluronan and cell surface CD44. J Biol Chem 2004;279:25745–25754
26. Smith-Garvin JE, Koretzky GA, Jordan MS. T cell activation. Annu Rev Immunol 2009;27:591–619
27. Brawand P, Fitzpatrick DR, Greenfield BW, Brasel K, Maliszewski CR, De Smedt T. Murine plasmacytoid pre-dendritic cells generated from Flt3 ligand-supplemented bone marrow cultures are immature APCs. J Immunol 2002;169:6711–6719
28. van Kooten C, Banchereau J. CD40-CD40 ligand. J Leukoc Biol 2000;67:2–17
29. Cella M, Scheidegger D, Palmer-Lehmann K, Lane P, Lanzavecchia A, Alber G. Ligation of CD40 on dendritic cells triggers production of high levels of interleukin-12 and enhances T cell stimulatory capacity: T-T help via APC activation. J Exp Med 1996;184:747–752
30. Coudronniere N, Villalba M, Englund N, Altman A. NF-kappa B activation induced by T cell receptor/CD28 costimulation is mediated by protein kinase C-theta. Proc Natl Acad Sci USA 2000;97:3394–3399
31. Sun Z, Arendt CW, Ellmeier W, et al. PKC-theta is required for TCR-induced NF-kappaB activation in mature but not immature T lymphocytes. Nature 2000;404:402–407
32. Trembleau S, Penna G, Gregori S, Gately MK, Adorini L. Deviation of pancreas-infiltrating cells to Th2 by interleukin-12 antagonist administration inhibits autoimmune diabetes. Eur J Immunol 1997;27:2330–2339
33. Trembleau S, Penna G, Bosi E, Mortara A, Gately MK, Adorini L. Interleukin 12 administration induces T helper type 1 cells and accelerates autoimmune diabetes in NOD mice. J Exp Med 1995;181:817–821

34. Ma L, Qian S, Liang X, et al. Prevention of diabetes in NOD mice by administration of dendritic cells deficient in nuclear transcription factor-kappaB activity. Diabetes 2003;52:1976–1985
35. Huet S, Groux H, Caillou B, Valentin H, Prieur AM, Bernard A. CD44 contributes to T cell activation. J Immunol 1989;143:798–801
36. Ilangumaran S, Briol A, Hoessli DC. CD44 selectively associates with active Src family protein tyrosine kinases Lck and Fyn in glycosphingolipid-rich plasma membrane domains of human peripheral blood lymphocytes. Blood 1998;91:3901–3908
37. Palacios EH, Weiss A. Function of the Src-family kinases, Lck and Fyn, in T-cell development and activation. Oncogene 2004;23:7990–8000
38. Ilangumaran S, Borisch B, Hoessli DC. Signal transduction via CD44: role of plasma membrane microdomains. Leuk Lymphoma 1999;35:455–469
39. Baranova NS, Nilebäck E, Haller FM, et al. The inflammation-associated protein TSG-6 cross-links hyaluronan via hyaluronan-induced TSG-6 oligomers. J Biol Chem 2011;286:25675–25686
40. Jaeckel E, Mpofu N, Saal N, Manns MP. Role of regulatory T cells for the treatment of type 1 diabetes mellitus. Horm Metab Res 2008;40:126–136
41. Madec AM, Mallone R, Afonso G, et al. Mesenchymal stem cells protect NOD mice from diabetes by inducing regulatory T cells. Diabetologia 2009; 52:1391–1399
42. Fiorina P, Jurewicz M, Augello A, et al. Immunomodulatory function of bone marrow-derived mesenchymal stem cells in experimental autoimmune type 1 diabetes. J Immunol 2009;183:993–1004
43. Tarbell KV, Petit L, Zuo X, et al. Dendritic cell-expanded, islet-specific CD4 + CD25+ CD62L+ regulatory T cells restore normoglycemia in diabetic NOD mice. J Exp Med 2007;204:191–201
44. Prockop DJ. Repair of tissues by adult stem/progenitor cells (MSCs): controversies, myths, and changing paradigms. Mol Ther 2009;17:939–946
45. Németh K, Leelahavanichkul A, Yuen PS, et al. Bone marrow stromal cells attenuate sepsis via prostaglandin E(2)-dependent reprogramming of host macrophages to increase their interleukin-10 production. Nat Med 2009;15: 42–49
46. Meisel R, Zibert A, Laryea M, Göbel U, Däubener W, Dilloo D. Human bone marrow stromal cells inhibit allogeneic T-cell responses by indoleamine 2,3-dioxygenase-mediated tryptophan degradation. Blood 2004;103:4619–4621
47. Groh ME, Maitra B, Szekely E, Koç ON. Human mesenchymal stem cells require monocyte-mediated activation to suppress alloreactive T cells. Exp Hematol 2005;33:928–934
48. Ortiz LA, Dutreil M, Fattman C, et al. Interleukin 1 receptor antagonist mediates the antiinflammatory and antifibrotic effect of mesenchymal stem cells during lung injury. Proc Natl Acad Sci USA 2007;104:11002–11007
49. Yagi H, Soto-Gutierrez A, Navarro-Alvarez N, et al. Reactive bone marrow stromal cells attenuate systemic inflammation via sTNFR1. Mol Ther 2010; 18:1857–1864
50. Gepts W, De Mey J. Islet cell survival determined by morphology. An immunocytochemical study of the islets of Langerhans in juvenile diabetes mellitus. Diabetes 1978;27(Suppl. 1):251–261